Wireless Flexible Strain Sensor Based on Carbon Nanotube Piezoresistive Networks for Embedded Measurement of Strain in Concrete

Fulvio Michelis, Laurence Bodelot, Costel-Sorin Cojocaru, Jean-Luc Sorin, Yvan Bonnassieux, Béreng ère Lebental

WIRELESS FLEXIBLE STRAIN SENSOR BASED ON CARBON NANOTUBE PIEZORESISTIVE NETWORKS FOR EMBEDDED MEASUREMENT OF STRAIN IN CONCRETE

F. Michelis[1-2], L. Bodelot[3], C.-S. Cojocaru[2], J.-L. Sorin[1], Y. Bonnassieux[2], B. Lebental[1-2]

1: Université Paris-Est, IFSTTAR, 14-20 bld Newton, 77447 Marne la Vallée, France
2: Laboratoire de Physique des Interfaces et Couches Minces (LPICM), UMR 7647, Ecole Polytechnique-CNRS, Route de Saclay, 91128 Palaiseau, France
3: Laboratoire de Mécanique des Solides (LMS), UMR 7649, Ecole Polytechnique-CNRS, Route de Saclay, 91128 Palaiseau, France

fulvio.michelis@ifsttar.fr

ABSTRACT

This work proposes a new type of low-cost strain sensor, based on piezoresistive carbon nanotube (CNT) network deposited on a flexible substrate. Experimental results show that the strain can be reliably measured thanks to the highly linear piezoresistive behaviour of the CNT network and thanks to temperature compensation capabilities. Moreover, the experimental results show the capability of measuring multiple loading cycles. The performance and the range of sensitivity of the device, suggest possible usage in the domain of embedded monitoring, in particular the detection of micro-strain and micro-cracking in concrete. In order to target this domain, a wireless RFID solution to embed the sensor into concrete is provided.

KEYWORDS: strain sensors, piezoresistivity, carbon nanotube, wireless monitoring, volume sensors.

INTRODUCTION

In the domain of structural health monitoring (SHM), strain gauges are traditionally exploited as surface sensors to monitor macro deformations of concrete structures [1] [2] [3]. The knowledge of macro deformations is used to assess the risk for structural failures [4]. Recent developments show that the use of strain gauges could be extended to micro scale for volume analysis of cracking [5] [6]. For instance, micro-cracking occurring near the reinforcement bars is symptomatic of alkaline reactions [7] [5]; more generally micro-cracking is associated with high porosity to chloride and other chemicals [8] [9] as well as general ageing [10].

In this work, we propose a new type of low-cost piezoresistive strain sensor that might offer a promising alternative to metallic strain gauges for volume monitoring of micro-strains and micro- cracking in concrete. The device has a linear piezoresistive response to mechanical deformations up to 10 µm, making the detection of micro-cracking, whose characteristic width is around 10 µm, theoretically possible [11]. Moreover, our solution is sensitive to stress in any direction, making it a good candidate for the detection of micro-fractures whose opening direction is arbitrary.

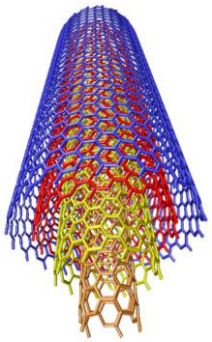

Figure 1 Model of a MWCNT [18]

According to the literature, our solution also provides the first evidence of a strain gauge fabricated by direct deposition of Carbon Nanotubes (CNTs) on polymer by inkjet printing. In addition, our approach allows the production of flexible strain gauges that can adapt better to complex configuration than metallic strain gauges. We propose a conditioning circuit and an RFID architecture to wirelessly power and communicate with the sensor embedded into concrete.

1. MODEL OF CNT STRAIN SENSING

Carbon nanotubes (CNTs) are hollow tubular structures with one or several concentric walls formed by one-atom-thick sheets of carbon (see Figure 1). The diameter of multi-walled nanotubes (MWNTs) is in the low nanometer range (5-50nm); their length is in the 5 µm to 50µm range. CNTs have been widely used for the exceptional electromechanical characteristics such as Young's modulus and electrical conductivity [12]. When deposited on a substrate, CNTs are organised in a grid, as shown in Figure 2. This grid can be modelled [13] as an electrical circuit in which the CNTs have a fixed resistance and the contacts between CNTs are modelled as tunnel resistances whose magnitude depends on the nanometric gap between two consecutive CNTs. The contact resistance can be modelled by $R_{tunnel} = a \cdot d \cdot e^{k \cdot d}$ (where a and k are constant values that define the material properties and d is the distance between the CNTs) (see Figure 2). When the network is strained, CNTs are expected not to elongate because of their high Young's modulus and the weak adhesion forces that bind them to the substrate. Consequently, the nanometric gap between adjacent CNTs increases, which translates into an increase in contact resistances. Globally, the increment of the contact resistances in the network induces an increment of the total resistance of the network. The influence of the mechanical deformation on the electrical resistivity of the CNT network, called piezoresistive behaviour, is at the basis of the strain detection mechanism analysed in this article.

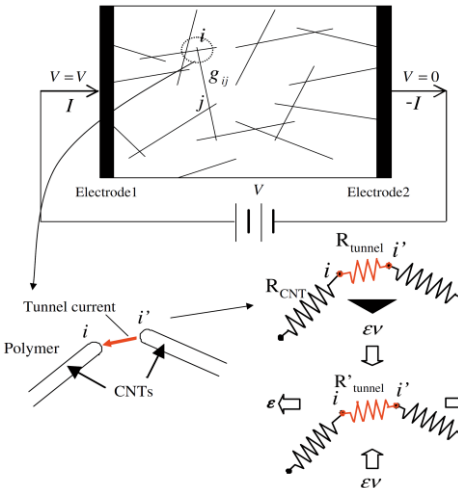

Figure 2 Electrical model of a CNT network [13]

2. EXPERIMENTAL PROCESS

2.1. Design of a CNT strain sensor

The substrate is a flexible polymer on which gold electrodes are deposited. The polymer is ETFE (Ethylene tetrafluoroethylene), is chosen for its high resistance to temperature, elevated pH and aggressive chemicals, and for its high resistivity. Gold is chosen for its high conductivity and high resistance to corrosion. A layer of CNTs is then deposited both on top of the contacts and between the electrodes. The size the device is: 5 x 17 mm (width x length) for a thickness of 0.15 mm (layout in **Error! Reference source not found.**3 and 4).

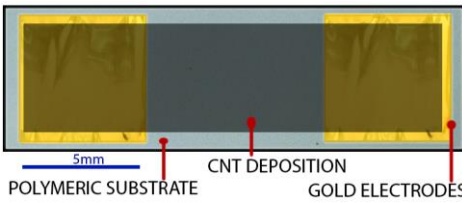

Figure 3 Layout of the CNT strain sensor

2.2. Materials and fabrication process

The substrate is acquired from Goodfellow (model FP361125, 0.125 mm thick). The gold electrodes are deposited by evaporation at room temperature. Their thickness is 100 nm. The CNTs are multiwalled CNTs C100 by Arkema Inc. To ensure device reproducibility and process scalability, CNT are deposited on the substrate by inkjet printing with a customizable Dimatix DMP-2800 printer (16 nozzles, 1pL printer head). To prepare the ink, the CNTs are dispersed in 1,2Dichlorobenzene at 0.02wt.% with SDBS additive at 0.3 wt.% using a ultrasonic probe for 20 minutes at 150W. CNTs in liquid solvents tend to form bundles. To remove the larger bundles,

which clot the cartridges, the solution is centrifuged at 10kG for 4h and the supernatants are extracted. The resulting solution is used as ink for the deposition. Printing is carried out keeping the substrate at 55°C and the cartridge at room temperature. The resistance of a single layer deposited on the substrate is very high due to lack of continuity of the network. Consequently, successive layers are printed. To further decrease the overall resistance of the deposition, it is rinsed every two deposited layers using an ethanol and acetone bath to remove solvent residues. A deposition of 20 layers was chosen as good compromise between fabrication time and gain in conductivity. A batch of 16 samples was fabricated at the same time, under the same environmental conditions. The average of the nominal resistances (resistance of the sensor prior to mechanical deformations) of the 16 samples is 200 kΩ and all the values were distributed at an interval of 100 kΩ around the mean. Such differences are relatively small and it can be possible to design a signal acquisition chain that adapts to these differences during an auto-calibration procedure at the beginning of the acquisition (section 5.1).

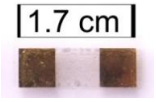

Figure 4: Layout of the fabricated device

3. CHARACTERIZATION

3.1. Traction bench

A 4-probe method is used to measure the resistance. The current applied to the system is generated by a Keithley 2612 (with 0.4% accuracy) and the voltage measurements are performed by the National Instrument acquisition card NI9212.

During the piezoresistive characterization, the sensors are positioned within a metallic frame, shielding them from electromagnetic noise. The deformation is achieved by gluing two extremities of the substrate to two clamps, mounted on force-controlled motors. The force control is achieved using the ALF328 load cell by Althen. A CCD camera is used to measure the local deformation of the substrate by following the displacement of surface patterns; the strains are deduced from the displacement. A thermocouple is used to monitor the environmental temperature at a distance of 1 cm from the side of the sample.

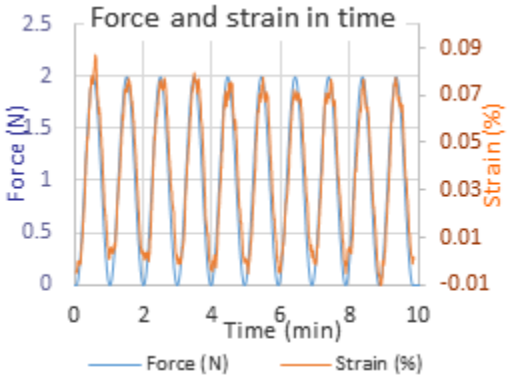

Figure 5 Cyclic load and resulting strain

3.2. Loading protocol

We studied the relationship between strain and resistance. In the linear regime, the sensitivity, called Gauge Factor (GF) and defined as the slope of the strain-resistance curve, was assessed.

In order to study the repeatability of the measurement over multiple loading cycles, a sinusoidal tensile stress was applied to the substrate with amplitude 2N and period 1 minute. Figure 5 shows the evolution of the force imposed on the system and the resulting strain of the polymeric substrate.

4. RESULTS

4.1. Single loading

The resistance/strain relationship is shown to be linear up to 2N and 600 microstrain (Figure 6), with GF=1.0 and R^2=0.99. Evident non-linearity occurs from 800 microstrain. Given that the size of the sample is 1.7 cm, a strain of 600 με induces a deformation of 10.2 μm.

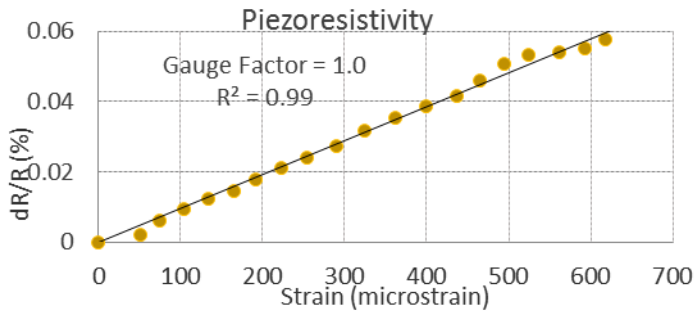

Figure 6: Piezoresistive behaviour of CNT strain sensor

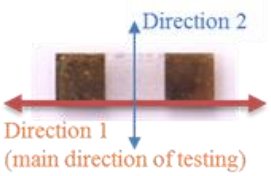

Figure 7 Direction of testing

The size of concrete micro-cracks responsible for chlorite permeability are as small as 10 µm [14] [15]. Consequently, the sensitivity to such deformations suggests the employability of this strain gauge for the early detection of micro-fractures in concrete. The results shown in Figure 6 represent the response to mechanical deformation which is parallel to the line electrodes-CNT-electrode (Direction 1 of Figure 7). Subsequently, the sensor was tested for perpendicular mechanical deformations and it showed the same sensitivity to strain; this behaviour is of interest because crack opening can occur in any direction and it might not be possible to control the orientation of the sensor after embedding in concrete [9] [11].

4.2. Cyclic load

The resistive response under cyclic loading is shown in Figure 8. The sensor response shows a significant downward drift towards smaller values. In order to understand the source of the drift and minimize its effect, the substrate deformation and the temperature were analysed. The elongation of the substrate was achieved by controlling the force between the clamps, but not the strain. Plastic deformation of the substrate was thus possible and could explain the drift. Similarly, the external temperature is an important factor to take into account since it affects both the substrate elasticity and the conductivity of the CNT network. Finally, the impact of the internal device temperature (caused by imposing a permanent current) was assessed.

Figure 9 displays the strain-force hysteresis for the substrate. The hysteresis is stable for the first 9 cycles, while the resistance drifts significantly; this suggests that plastic deformations are not responsible for the drift in resistance.

The temperature at 1 cm from the sensor was analysed (Figure 11). The average of the temperature and the average of the resistance were calculated for each cycle (Figure 10) reports on the evolution of the resistance and of the temperature vs. cycle number. Though the tendency is not obvious, there may be a global downward drift of the temperature which may explain the drift in resistance. To confirm this, the temperature dependence of the resistance is assessed. Figure 12 shows the influence the temperature has on 3 different sensors; this result is particularly important because it shows that different sensors react the same way to temperature and, consequently, it is possible to extrapolate the so-called temperature coefficient of resistance α_{temp}=-0.12, an important parameter in the compensation of temperature changes. In fact, if a control sensor not subject to mechanical deformation is added to the system, it is possible to subtract the drift of the control sensor (drift due to the temperature change) from the reading of the sensor subject to both strain and temperature change. It is known that the resistance of a sensor subject to strain and temperature change is $R = R_0(1 + \alpha_{temp} \cdot \Delta T + GF \cdot \varepsilon)$ where R_0 is the resistance at the temperature of reference, α_{temp} is the coefficient linking temperature change to resistance change, ΔT is the temperature change from the reference value, GF is the gauge factor and ε is the strain. If the coefficient α is the same for every sensor, it is then sufficient to subtract the relative change of resistance of the control sensor from the resistance of the strain sensor to obtain a temperature-compensated measurement.

Figure 13 shows the improvement of the measurement due to the temperature compensation. Further study is required to understand the source of the remaining drift.

4.3. Reproducibility

To address real-life application one key requirement to fulfil is the reproducibility, defined as the ability to perform the same measurement with different sensors. To evaluate the reproducibility, four sensors were tested at the same time, under the same mechanical deformation and exposed to the same environmental conditions. The four sensors were tested for multiple cycles. One of the sensors shows a considerably different behaviour compared to the others, but the sensors 2 to 4 show analogous behaviour, especially for the first three cycles (Figure 14). This promising result suggests that reproducibility can be obtained. Further investigation is needed to identify the cause of the divergence of one of the sensors.

5. EMBEDDED MONITORING IN CONCRETE

In order to target the domain of SHM, a smaller and cheaper way to read the sensor is needed. Moreover, since the sensor will be cast into concrete, the solution provided must be capable of collecting power supply and communicating wirelessly through concrete. In fact, the use of wired technology is excluded since the cables would create a breach for the entrance of chemicals potentially dangerous to concrete. In the following paragraph we present the work done in the design of the electronic system. The architecture presented is currently under production and has not been tested yet in situ.

5.1. Acquisition chain

For preliminary tests a simple acquisition chain, based on a Wheatstone bridge, is developed. The purpose of this chain is the translation of a change in resistance into a change in voltage, which will be converted to a digital value with an Analog to Digital Converter (ADC). Figure 15 shows the acquisition chain developed. It is possible to identify four different sections: the Wheatstone bridge to convert the resistance change into a voltage, an instrumentation amplifier to provide gain, a filter and the ADC. The Wheatstone bridge and the amplifier exploit a potentiometer to adjust to the differences in the nominal resistance

5.2. Wireless communication and power supply

Wireless communication can be achieved using several communication protocols such as Bluetooth, WiFi and ZigBee, but for the presented work, RFID seems to be the optimal solution since it allows wireless power supply over Radio Frequency, along with communication capabilities. In fact, RFID modules are designed in such a way that when the antenna is not in communication state, the power collected by the antenna is stored in a capacitor. The RFID system is based on two modules: the reader and the tag. In this work we propose a system in which the reader is outside the concrete structure and wirelessly interrogates the tag inside the structure that has sensing capabilities. The tag, receiving energy from the reader by electromagnetic waves, is activated, performs strain measurements and communicates the acquired information. The architecture is shown in Figure 16.

CONCLUSIONS

We have developed a polymer-carbon nanotube based strain gauge and we have proved the capability of the sensor to detect deformations comparable to the deformations found in micro-cracking in concrete. We demonstrated the possibility of compensating for temperature changes and we have obtained highly promising results on the reproducibility of the measurement. Future work will be focused on boosting the performance and the repeatability. With the architecture under fabrication, in situ trials will be performed to analyse the behaviour of the sensor in real life applications.

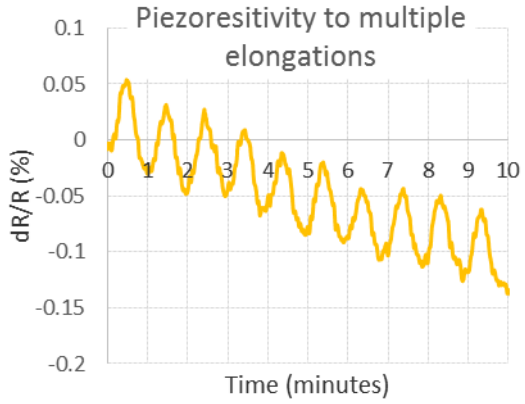

Figure 8 Response to multiple and repetitive loading cycles

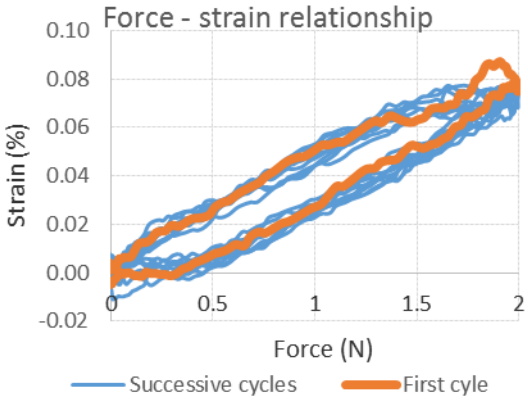

Figure 9 Relationship between the force imposed on the system and the resulting strain

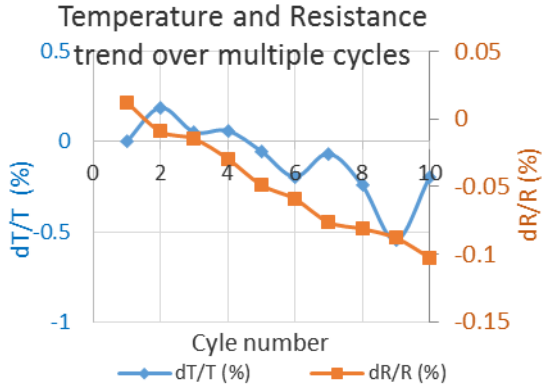

Figure 10 Average change of resistance and temperature per cycle. The average of the first cycle is taken as a reference value from which the variation dT is calculated.

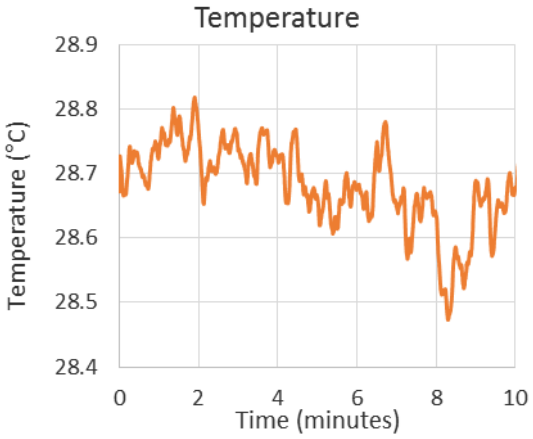

Figure 11 Temperature of the air surrounding the sensor under study

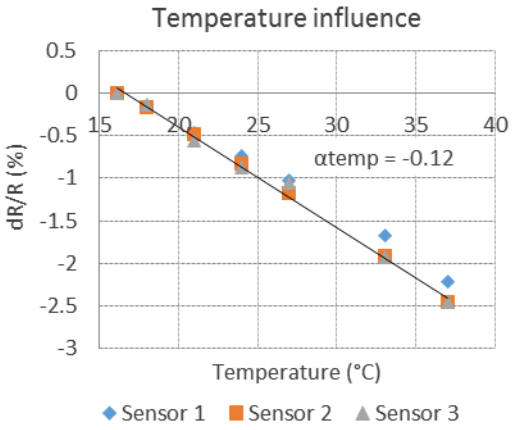

Figure 12 Influence of temperature over the resistance

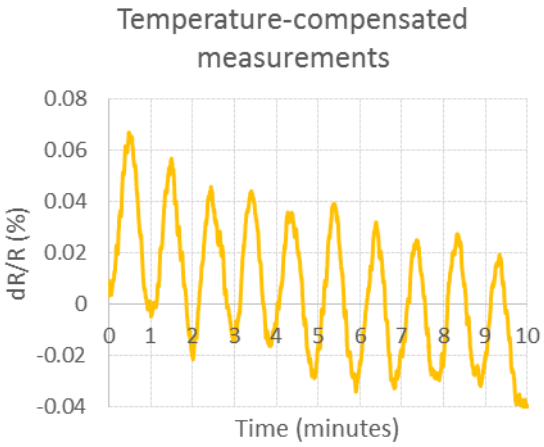

Figure 13 Temperature-compensated piezoresistivity measurement over multiple loading cycles.

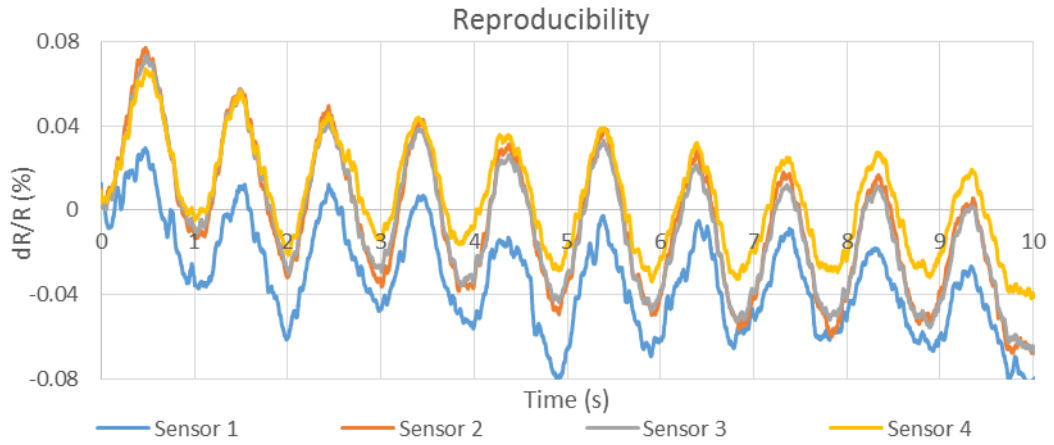

Figure 14 Study of the reproducibility of the measurement. Four sensors characterized at the same time. The results are temperature-compensated

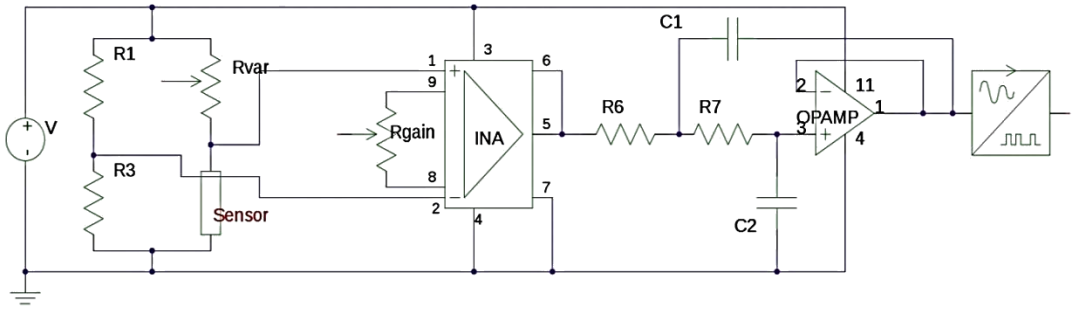

Figure 15 Acquisition chain to translate the resistance change in voltage change

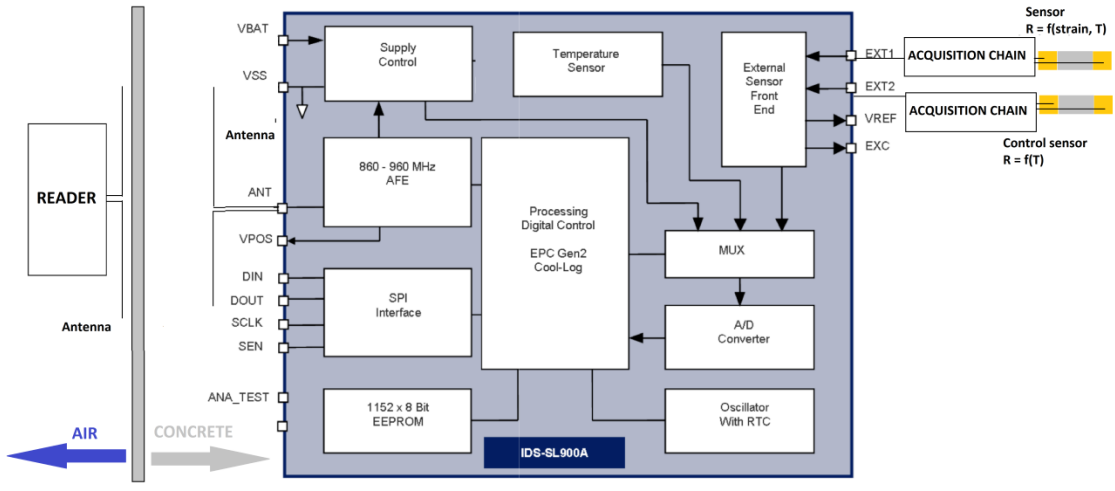

Figure 16 RFID architecture (schema of the SL900A taken from [16])

REFERENCES

[1] K.-y. Wong, C. K. Lau et A. R. Flint, «Planning and implementation of the structural health monitoring system for cable-supported bridges in Hong Kong,» *Proceedings to Nondestructive Evaluation of Highways, Utilities, and Pipelines IV,* 2000.

[2] H. Wenzel, Health Monitoring of Bridges, Wiley, Éd., 2009.

[3] L. H, J. Ou, X. Zhao, W. Zhou, H. Li et Z. Zhou, «Structural Health Monitoring System for the Shandong Binzhou Yellow River Highway Bridge,» *Computer-Aided Civil and Infrastructure Engineering,* pp. 306-317, 2006.

[4] C. Haksoo, «Structural Health Monitoring system based on strain gauge enabled wireless sensor nodes,» *Proceedings to Networked Sensing Systems, 2008,* 2008.

[5] G. Batis et T. T. Routoulas, «Data analysis of strain gauges detecting steel rebars corrosion,» *Proceedings to the Interantional Conference on Concrete Durability and Repair Technology,* pp. 563-572, 1999.

[6] P. Poornachandra, V. Ansal, K. Venkataramana et P. Parthiban, «Experimental investigation on corroded reinforced concrete beam in coastal environment using strain gauges,» *International Journal of Engineering and Innovative Technology,* 2013.

[7] V. M. Sounthararajan et A. Sivakumar, «Corrosion Measurements in Reinforced Fly Ash Concrete,» *International Journal of Corrosion,* 2013.

[8] M. Farage, J. Alves et E. Fairbairn, «Macroscopic model of concrete subjected to alkali–aggregate reaction,» *Cement and Concrete Research,* pp. 495-505, 2004.

[9] C. Lim, N. Gowripalan et V. Sirivivatnanon, «Microcracking and chloride permeability of concrete under uniaxial,» *Cement & Concrete Composites,* pp. 353-360, 2000.

[10] Z. Yang, W. Weiss et J. Olek, «Interaction Between Micro-Cracking, Cracking, and Reduced Durability of Concrete: Developing Methods for Considering Cumulative Damage in Life-Cycle Modeling,» Purdue University, West Lafayette, Indiana, 2004.

[11] P. Grassl, H. Wong et N. Buenfeld, «Influence of aggregate size and volume fraction on shrinkage induced micro-cracking of concrete and mortar,» *Cement and Concrete Research,* 2010.

[12] E. T. Thostenson, Z. Ren et T.-W. Chou, «Advances in the science and technology of carbon nanotubes and their composites: a review,» *Composites Science and Technology,* vol. 61, n° %113, 2001.

[13] N. Hu, Y. Karube, M. Arai, T. Watanabe, C. Yand, Y. Li, Y. Liu et H. Fukunaga, «Investigation on sensitivity of a polymer/carbon nanotube composite strain sensor,» *Carbon,* vol. 48, n° %13, 2010.

[14] X. H. Shi et X. Shi, «Chloride Permeability and Microstructure of Portland Cement Mortars Incorporating Nanomaterials,» *Journal of the Transportation Research Board,* 2008.

[15] J. Zheng, H. Wong et N. Buenfeld, «Assessing the influence of ITZ on the steady-state chloride diffusivity of concrete using a numerical model,» *Cement and Concreat Researches,* 2009.

[16] IDS_Microchip, *SL900A Datasheet,* 2010.

[17] M. Hoseini, V. Bindiganavile et N. Banthia, «The effect of mechanical stress on permeability of concrete: A review,» *Cement & Concrete Composites,* pp. 213-220, 2009.

[18] University of Surrey, [En ligne]. Available: http://www.ph.surrey.ac.uk/newsite/profile_images/Smith2006Feb14161240.png. [Accès le 16 04 2014].

[19] K. A. T. Vu et M. G. Stewart, «Structural reliability of concrete bridges including improved,» *Structural Safety,* pp. 313-333, 2000.